Diffusion and Partitioning of Solutes in Agarose Hydrogels: The Relative Influence of Electrostatic and Specific Interactions

Nicolas Fatin-Rouge,* Antoine Milon, and Jacques Buffle

Laboratory of Analytical and Biophysical Environmental Chemistry, Sciences II, University of Geneva, 30 Quai E. Ansermet, CH-1211 Geneva 4, Switzerland

Richard R. Goulet and André Tessier

INRS-ETE, University of Quebec, C.P. 7500 Sainte-Foy Quebec, Canada

Received: March 10, 2003; In Final Form: August 13, 2003

The nature and density of charged sites in an agarose gel have been studied. Diffusion and partition coefficients of various organic and inorganic ions have been measured as a function of ionic strength, μ, and pH to investigate the solute−gel interactions resulting from charge effects and specific complexation. The majority of binding sites in the gel are pyruvate groups, with an intrinsic protonation constant of $\log K_a^{int} = 3.9$. We measured the charge density of the gel as a function of added salt and pH and evaluated the Donnan potential. The partition coefficients of cations decrease and those of anions increase with increasing ionic strength because of progressive screening of the anionic sites in the gel, as predicted by the Boltzmann and Poisson−Boltzmann equations. The charges in the gel become completely screened at $\mu \approx 10^{-2}$. As predicted with the Smoluchowski−Poisson−Boltzmann theory, the diffusion coefficient of cationic species is reduced at low ionic strength. We tested both cylindrical and spherical symmetries of Poisson−Boltzmann cell models to describe these variations and obtained better results with the former. In addition to electrostatic effects, we detected specific interactions between metal ions and the gel, and we determined the intrinsic association constants. General models are presented for the partitioning and diffusion of solutes in the gel, which consider steric, electrostatic, and chemical interactions.

1. Introduction

Understanding solute−gel interactions is of importance for many applications of gels. Numerous analytical separation or preconcentration methods (e.g., diffusion gradient in thin films (DGT),[1] gel electrophoresis,[2] and voltammetric gel integrated microelectrodes[3,4]) require the controlled diffusion of solutes in organic gels. Diffusion in gels is also an important component in many environmental,[5] pharmaceutical,[6] and biological[7] applications of gels. Under non-steady-state conditions, the diffusion of solutes may be significantly affected by their specific and nonspecific interactions with the gel fibers; these interactions should be well understood if solute diffusion is to be controlled.

Agarose is a linear polysaccharide consisting of repeating units of agarobiose (1, 3-linked β-D-galactopyranose and 1, 4-linked 3,6-anhydro-α-L-galactopyranose); it is isolated from agar, which is obtained from marine red algae (*Rhodophyta*). The main ionic chemical moieties usually present in the agarobiose backbone are sulfonate, ester sulfate, ketal pyruvate, and carboxyl groups located at the 2 and 6 positions of β-D-galactopyranose.[8,9] The amount of these impurities can affect the physicochemical properties of agarose hydrogels.[10] By cooling a hot solution of agarose in water, double helixes[11] are formed by the association of the polymer chains, resulting in a 3D network that entraps the solvent to produce a gel[12] through hydrogen bonding and hydrophobic interactions. Agarose gels are weakly ionic, with a pore-size distribution ranging from 1 to 900 nm, depending on the agarose concentration.[13] The wide pore-size distribution has been demonstrated by using neutron scattering,[14] transmission electron microscopy (TEM),[15] and atomic force microscopy (AFM).[16] Neutron-scattering measurements have shown a broad range of pore sizes (1−480 nm) for the agarose hydrogel used in this study. [14]

The hindered diffusion of solutes in gels has been modeled[17,18] and is well documented for agarose gels.[19,20] For instance, agarose hydrogel is the preferred chromatographic medium used for separating biological molecules of molecular weight greater than 250 KDa, for which minimal nonspecific binding and retention of the biological activity of the molecules are required. However, the diffusion and partitioning of charged solutes, particularly small ions, in charged gels is largely unknown and deserves further investigation. There have been only a few systematic physicochemical studies on the interactions of charged solutes with agarose gels and how they affect their diffusion; these studies involved large molecules and did not reach clear conclusions. For example, Zhang et al.[21] investigated the diffusion and adsorption of bovine serum albumin (BSA) and lysozyme in cibacron blue 3GA modified agarose gels at ionic strengths (μ) ranging from 0.01 to 0.3 and concluded that there are variations in the diffusion coefficient of BSA with μ. In another study, Johnson et al.[22] investigated the diffusion and partitioning of fluorescein-labeled proteins in 6% sulfated-agarose hydrogels at pH 7 and μ ranging from 0.01 to 1 using the fluorescence recovery after photobleaching technique (FRAP); they concluded that there is no theory that relates the apparent

* To whom correspondence should be addressed. E-mail: nicolas.fatin-rouge@wanadoo.fr.

10.1021/jp0303164 CCC: $25.00
Published on Web 10/10/2003

diffusion coefficients to partition coefficients. However, interpreting their results is difficult because at pH 7, even if the net charge of the diffusing proteins is negative they have positively charged moieties. This latter study emphasizes the need to select simple positively or negatively charged solutes to probe the electrical interactions with charged gels accurately. Hirota et al.[23] studied the effect of intrinsic charges on the diffusion of myoglobin (size = 4.5 nm × 3.5 nm) in agarose and λ-carrageenan gels; they reported an electrostatic interaction for λ-carrageenan gel but not for agarose gels at $\mu \geq 0.04$. Mattisson et al.[24] investigated how electrostatics affect the mass transfer of lysozymes in agarose gels and modeled the protein−protein interactions as a function of μ and pH by applying the Poisson−Boltzmann (PB) cell model. Recent applications of the DGT technique[1] for measuring metal concentrations in natural waters[25] also indicated abnormally high diffusion coefficients and significant interactions of Cd^{2+} in hydrogels at $\mu < 10^{-3}$.[26]

The diffusion of solutes has also been studied in polymer solutions. Phillies et al.[27,28] reported an exponential decrease in the diffusion coefficients of polystyrene latexes in poly(acrylic acid) solutions with decreasing μ. Also, it has been shown for several decades that the electrostatic field set up by the fixed charges of polyions influences the transport properties of other ions in solution.[29,30] The self-diffusion of counterions is slower in a solution containing a polyelectrolyte than in others containing only simple electrolytes because of the strong local electrostatic field originating from the high charge density of the polymer. The Smoluchowski−Poisson−Boltzmann (SPB) theory describes molecular diffusion in electrical environments and can be applied to media such as gels. The SPB theory considers the 3D local symmetry and periodicity of the electric field in the medium. For example, the PB equations in spherical or cylindrical cells were used to model the diffusion of ions in media containing oppositely charged micellar,[31,32] colloidal,[33] or polymeric[34] particles, assuming that diffusing ions cannot penetrate inside the particles and that charges are uniformly distributed on the particles' surfaces. Finally, Johansson et al.[35] have recently modeled the diffusion of monovalent ions in oppositely charged gels by using Monte Carlo simulations with a modified Debye−Hückel equation.

In this study, we mainly investigated the diffusion and binding properties of an agarose gel, and we interpret the data with models describing solute diffusion in this hydrogel that account for the electrical, steric, and chemical interactions.

2. Theory

2.1. Distribution of Solutes Between the Agarose Gel and an Aqueous Solution. The distribution of solute A between a charged agarose hydrogel and water can be described by a global partition coefficient, Φ:

$$\Phi = \theta\alpha\pi = \frac{[A]_g}{[A]_w} \tag{1}$$

where θ, α, and π are the partition coefficients for purely steric, chemical, and electrostatic interactions, respectively, and $[A]_g$ and $[A]_w$ are solute concentrations in the gel and in the external water at equilibrium, respectively.

Steric Interactions. When all pores have the same radius R_p, θ can be calculated for spherical molecules or particles of $R_A < R_p$ using the equation[36]

$$\theta = (1 - \phi) \times \left(1 - \frac{R_A}{R_p}\right)^2 \tag{2}$$

where R_A is the solute hydrodynamic radius and ϕ is the volume fraction of polymer in the hydrogel. Equation 2 is not rigorously applicable to agarose hydrogels that have a broad distribution of pore sizes, but it allows us to estimate θ.

Electrostatic Interactions. The agarose gel contains ionizable groups that can be negatively charged (section 4.1), and π can be described by a Boltzmann distribution

$$\pi = \exp\left(-\frac{z_A F\psi}{RT}\right) \tag{3}$$

where z_A is the electrical charge of A, ψ is the average difference in potential (Donnan potential) between the gel and the external solution, F is the Faraday constant, R is the gas constant, and T is temperature. The Donnan potential in the agarose gel is related to its charge density (ρ), the molar concentration (c) of the electrolyte (assumed to be symmetrical) in the external solution, and the charge (z) of the cation or anion of the electrolyte by the following relationship:[37]

$$\psi = \frac{RT}{zF} \sinh^{-1} \frac{\rho}{2zFc} \tag{4}$$

In turn, the charge density (ρ; C/kg) is related to the concentration of negatively charged groups (Q) within the gel:

$$\frac{|\rho|}{F} = Q \tag{5}$$

Specific Chemical Interactions. When solute A reacts with sites S of the hydrogel to form a complex SA, Φ is expressed as follows (assuming $\theta = 1$):

$$\Phi = \frac{[A]_g}{[A]_w} = \frac{[A]_p + [SA]}{[A]_w} \tag{6}$$

where $[A]_p$ and [SA] are the concentrations of A in the pore water of the gel and bound to sites S of the gel, respectively.

The intrinsic equilibrium constant, K_A^{int}, for the formation of SA into the gel, under conditions where $\psi = 0$, is given by

$$K_A^{int} = \frac{[SA]}{[A]_p[S]} \tag{7}$$

where [S] is the concentration of free sites. When $\psi \neq 0$, $[A]_p = [A]_w \exp(-z_A F\psi/RT)$ and eq 7 becomes

$$K_A^{int} = \frac{[SA]}{[A]_w[S] \exp\left(-\frac{z_A F\psi}{RT}\right)} = K_A^{app} \exp\left(\frac{z_A F\psi}{RT}\right) \tag{8}$$

where K_A^{app} is an apparent equilibrium constant that includes charge effects. Combining eqs 3, 6, and 8 gives

$$\Phi = \exp\left(-\frac{z_A F\psi}{RT}\right)(1 + K_A^{int}[S]) = \pi\alpha \tag{9}$$

When $\theta = 1$ and $\psi = 0$ ($\pi = 1$), eq 9 reduces to

$$\Phi = \alpha = 1 + K_A^{int}[S] \tag{10}$$

2.2. Diffusion of a Solute within the Agarose Gel. The ratio (σ) of the diffusion coefficient of solute A in the gel pores when only steric effects are important (D_p) to that in water (D_w) can be calculated according to Renkin's model, which describes the

restricted diffusion of spherical molecules within cylindrical pores as[38]

$$\sigma = \frac{D_p}{D_w} = 1 - 2.1444 \times \frac{R_A}{R_p} + 2.08877 \times \left(\frac{R_A}{R_p}\right)^3 - 0.94813 \times \left(\frac{R_A}{R_p}\right)^5 - 1.372 \times \left(\frac{R_A}{R_p}\right)^6 + 3.87 \times \left(\frac{R_A}{R_p}\right)^8 - 4.19 \times \left(\frac{R_A}{R_p}\right)^9 \quad (11)$$

2.2.1. Macroscopic Description. When an agarose gel separates two solutions of different concentrations of solute A (as in a diffusion cell; see section 3.3), solute A diffuses through the gel from the more concentrated (source) to the less concentrated (receiving) solution. After an initial induction period, a steady-state regime is established, and a linear concentration gradient, $d[A]_g/dx$, is set up within the gel. The flux (J; mol cm^{-2} s^{-1}) of A within the hydrogel is given by Fick's first law:

$$J = \bar{D}_g^A \times \frac{d[A]_g}{dx} \quad (12)$$

where $\bar{D}_g^A$ (cm^2 s^{-1}) is the average diffusion coefficient of A within the gel. Equation 12 can be rewritten as

$$J = \frac{\bar{D}_g^A([A]_g^s - [A]_g^r)}{m} \quad (13)$$

where m is the gel membrane thickness and $[A]_g^s$ and $[A]_g^r$ are the total concentrations of A in the gel at the gel/source and gel/receiving solution interfaces, respectively. The partition coefficient of A at both interfaces of the hydrogel includes sterical (θ), chemical (α), and electrostatic (π) interactions and is given by eq 1, which can be rewritten as

$$\Phi = \theta\alpha\pi = \frac{[A]_g^s}{C_s^A} = \frac{[A]_g^r}{C_r^A} \quad (14)$$

where C_s^A and C_r^A are the concentrations of A in the bulk source and receiving solutions, respectively, provided that the diffusion boundary layer thicknesses at both interfaces are negligible. Combining eqs 13 and 14 gives

$$J = \frac{\theta\alpha\pi\bar{D}_g^A(C_s^A - C_r^A)}{m} = \frac{\Phi\bar{D}_g^A(C_s^A - C_r^A)}{m} \quad (15)$$

The average diffusion coefficient of A within the gel, $\bar{D}_g^A$, in the absence of an electric field effect is given by[39]

$$\bar{D}_g^A = \frac{D_p^A}{\alpha} + \frac{D_g^{SA}(\alpha - 1)}{\alpha} \quad (16)$$

where D_p^A is the diffusion coefficient of A in the pores for the water of the gel and D_g^{SA} is that of the complex SA in the gel. Combining eqs 11 and 16 and assuming that $D_g^{SA} = 0$ (because sites S are fixed on the agarose fibers), one obtains

$$\bar{D}_g^A = \frac{\sigma D_w^A}{\alpha} \quad (17)$$

Combining eqs 15 and 17, one gets

$$J = \frac{dN}{S_m\,dt} = \frac{\Phi\bar{D}_g^A(C_s^A - C_r^A)}{m} = \frac{\sigma\theta\pi D_w^A(C_s^A - C_r^A)}{m} \quad (18)$$

where N is the number of moles of A diffusing at time t and S_m is the gel's surface area. Equation 18 shows that flux J is independent of α under steady-state conditions (i.e., after the induction period (or time lag)). Integrating eq 18 over time for conditions where the depletion of A in the source solution remains negligible provides N:

$$N = \frac{S_m\Phi\bar{D}_g^A C_s^A t}{m} = \frac{S_m\sigma\theta\pi D_w^A C_s^A t}{m} \quad (19)$$

The products $\Phi\bar{D}_g^A$ and $\sigma\theta\pi$ can be obtained from the slope, s, of the linear plot of N versus time.

Equation 19 is based on the assumption that A forms a specific complex, SA, with sites S of the gel, whose strength is described by the equilibrium constant K_A^{int} (comprising the α term in eqs 15−17; see eq 10) and that, in addition, it is attracted by or repulsed from the gel because of its electric field (term π in eq 15).

2.2.2. Microscopic Description. In eqs 18 and 19, however, the π term takes into account only the effect of the gel's electric field on the average partitioning of A between the solution and the gel without describing its effects on the diffusion of A within the gel. According to the SPB theory, the diffusional flux of ions within an electric field is expressed for the steady state by the equation

$$J = -D_g^A(\nabla[A]_p + z_A[A]_p\nabla\Psi) \quad (20)$$

where $[A]_p$ is the local concentration of solute A in the pores within the gel and $\Psi(r) = F\,\psi(r)/RT$ is the local reduced electrostatic potential set up by the charged agarose fibers. It is assumed that $[A]_p$ is averaged over macroscopic distances (greater than micrometers) but is allowed to vary locally (1−100 nm) because of inhomogeneity in concentrations generated by the charged fibers. From the average electrolyte concentration in the pores of the gel, the concentration profile of ions surrounding a charged volume and thus the corresponding $\Psi(r)$ can be estimated with a PB-cell model,[40] where the agarose fibers are assumed to be homogeneously distributed in the gel and surrounded regularly by others fibers. Two geometric cells (cylindrical and spherical; see Scheme 1) have been tested in the model.

SCHEME 1

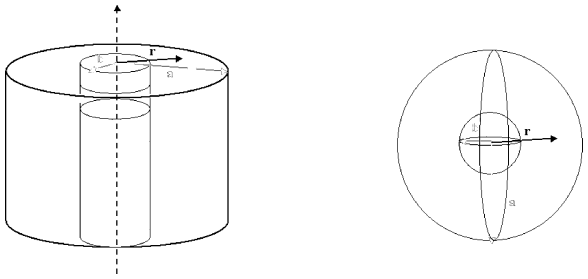

Cylindrical Cell. The cylindrical cells represent the geometric form of the charged volume for a linear polymer. Two sets of geometrical parameters, a and b, have been tested (see Scheme 1). First, we reproduce the fiber fraction of the hydrogel solution, ϕ, by $\phi = b^2/a^2$ or the geometric characteristics (i.e., $R_p = a - b$ is the average pore radius, and b is the average fiber radius R_f) that have been experimentally determined (see sections 4.1,

4.4, and 4.5). The calculated[41] volume fraction of the agarose hydrogel is $\phi = 1.317 \times 10^{-2}$. We considered that the negative charges of agarose are spread over the fibers' surface. According to Nilsson et al.[34] for an infinitely small solute in the absence of specific interaction, the ratio D_g^A/D_w^A is given by the following expression:

$$\frac{D_g^A}{D_w^A} = \frac{1}{3} + \frac{\frac{2}{3}\chi(a)}{e^{-z_A\Psi(r)}} \quad (21)$$

where $\chi(r)$, is a function of the distance, r, from the center of the cylinder and $\Psi(r)$ is obtained by solving the differential equation. (Note that in the original article[34] there is a typographical error in this equation.)

$$\frac{d\chi(r)}{dr} + \chi(r) \times \left(\frac{\chi(r)}{r} - z_A\frac{d\Psi(r)}{dr}\right) - \frac{1}{r} = 0 \quad (22)$$

for $\chi(a)$, with the boundary condition $\chi(b) = 0$.

Spherical Cell. Given the relatively small charge density of the agarose gel and its fractal structure, we assume that nonmobile charges are homogeneously distributed within the bulk of the gel. From the gel's charge density, a mean distance between two anionic site of 22 nm is calculated (see section 4.1). We assume that each negative charge of the agarose polymer is spread over the surface of a sphere of radius b embodied within a spherical cell of radius a (set equal to 11 nm, which is half the distance between two anionic sites). The value of b was obtained either from the value of ϕ or from the measurement of the agarose fiber radius (see section 4.1). According to Bell,[31,32] the ratio D_g^A/D_w^A is given by the following expression:

$$\frac{D_g^A}{D_w^A} = \frac{\chi(a)}{e^{-z_A\Psi(r)}} \quad (23)$$

where $\Psi(r)$ is obtained by solving the differential equation

$$r\frac{dc(r)}{dr} + \chi(r) \times \left(1 + \chi(r) - rz_A\frac{dY(r)}{dr}\right) - 2 = 0 \quad (24)$$

for $\chi(a)$ with the boundary condition $\chi(b) = 0$.

In practice, for both cells, $\Psi(r)$ was obtained first by solving the Poisson−Boltzmann equation numerically using the PB-cell model.[24,40] The function $\Psi(r)$ was then accurately fitted in the range $r = [b; a]$ with a polynomial function (sixth order) that was introduced in eq 22 or 24 and then numerically solved to obtain $\chi(a)$ with the Mapple program using a fourth-order Runge−Kutta procedure. Admittedly, a more sophisticated description of the system would be needed to account for the pore-size distribution in the gel for the real size of the solutes as well as for their chemical interactions with agarose. For example, Nilsson noted that the upper limit of the ratio D_g^A/D_w^A, calculated when $\psi = 0$, is $(D_g^A/D_w^A)_{\psi=0} = (1/3) + (2/3)/(1 + \phi)$ (i.e., $(D_g^A/D_w^A)_{max} = 0.991$ here). In this work, the diffusing solutes investigated in a variable electric field are small compared to the mean pore radius, R_p, and such a correction factor can be omitted. However, it is realistic to introduce a multiplying correction factor $\gamma = 1/\alpha$ into eqs 21 and 23 to account for chemical interactions.

The above considerations suggest that three types of factors should be studied to understand the partitioning of solutes between an agarose gel and the external solution and their diffusion within the gel: the electrical effects expressed as π and $\psi(r)$, the chemical interactions described by α, and the steric factors expressed as θ and σ. Because the steric effects have been studied for agarose gels,[41] this study emphasizes the other two factors. We focus on the diffusion and partitioning of small rigid and charged solutes ($R_A \leq 1$ nm), which should minimize hindering and size-dependent salt concentration effects. We are aware that some models used here (e.g., eq 2 and the SPB theory with the cylindrical and spherical cells) are not rigorously applicable to the agarose gel because of its complex structure, but despite their limitations, these models allow a semiquantitative evaluation of the importance of different factors in the absence of more rigorous theories.

3. Experimental Section

3.1. Reagents and Gel Preparation and Characterization. Purified agarose (LGL, molecular biology grade,lot no. 8041) obtained from Biofinex (Switzerland) was used without further purification. Pyruvic acid and sulfur contents reported by Biofinex are 0.2 and 0.02% respectively. We determined a value of $(1.9 \pm 0.2) \times 10^{-2}$ %S by hydrolyzing 5 g of dried agarose with HNO_3 at 90 °C for 4 h, by adding formaldehyde to the hot solution until red fumes disappeared, and by measuring S gravimetrically as $BaSO_4$.[42] Moisture (10.2%) was measured by the Karl Fischer test.

Fluorophores (see Scheme in Supporting Information for chemical structures) rhodamine 6G (R6G, Sigma 99%), calcein (Molecular Probes, high purity), eosin yellow (Fluka, puriss), Nile blue (Across), and LiF (Fluka) were of analytical grade. Humic acids (Suwannee River humic acid, HA, and peat standard humic acids 1S103H, peat HA) were obtained from the International Humic Acid Substances Society. Four fluorescent proteins (codfish parvalbumin, ovalbumin, allophycocyanin, and *R*-phycoerythrin) were obtained from Molecular Probes. Stock solutions of HTO (Dupont NEN product) and ^{109}Cd (Pharmacia Biotech; in 0.1 M HCl) were diluted 10× and 200×, respectively, with water to obtain suitable activities for spiking during diffusion experiments. μ was adjusted with NaCl (BDH AnalaR) or $NaNO_3$ (Merck, suprapur). Ultrapure water (>18 MΩ cm) was used to prepare all solutions.

The agarose gel (1.35% once corrected for the water content of the agarose polymer) was prepared by dissolving 1.5 g of agarose in preheated ultrapure water (between 90 and 100 °C) to a final volume of 100 mL. The solution was covered and heated for 40−60 min; the clear solution was transferred into preheated (70 °C) gel-casting assemblies and left to cool to its gelling temperature (below 37 °C). For the diffusion measurements by fluorescence correlation spectroscopy (FCS), the fluorophores (typically 2×10^{-8} M) were introduced into the gel solution before its gelification. Gel thickness was measured by optical microscopy.

An infrared spectrum of agarose incorporated into KBr pellets was obtained by Fourier transform infrared (FTIR) spectroscopy (Mattson Alpha Centauri); the spectra were recorded between 4000 and 400 cm^{-1}. Differential scanning calorimetry (DSC; Perkin-Elmer, model DSC-7) was used to investigate the nature of water within the agarose gel. The calibration for temperature and enthalpy was done with indium. A piece of gel, prepared and stored in ultrapure water, was placed in a sealed aluminum pan, cooled to −50 °C with liquid nitrogen, and then heated to 30 °C at a rate of 5 °C min^{-1}. The melting peak of water observed around 0 °C was used to calculate the amount of freezable water using the enthalpy of fusion of water (6.008 kJ mol^{-1}).[43]

3.2. Measurement of Diffusion Coefficients by FCS. Diffusion coefficients of dyes within the gel were measured by fluorescence correlation spectroscopy (FCS; ConfoCor Axiovert 135 TV; Carl Zeiss) using confocal microscopy. Typically, 0.5 mL of a gel solution (60 °C) was introduced into a hole (dimensions are about $0.9 \times 0.9 \times 0.9$ cm^3) of the FCS cell and left to cool for gelification, giving a roughly cubic piece of gel; alternatively, for measurements of diffusion coefficients versus pH, small cubic pieces of gel (dimensions were about $0.5 \times 0.5 \times 0.5$ cm^3), preequilibrated for 1 h in a buffer solution, were placed into the FCS cell. The gel samples were excited with an Ar^+ laser (488 or 514 nm) or a He/Ne laser (545 nm), and the fluorescence intensity was measured with an avalanche photodiode detector (SPCM-200PQ). The variations in fluorescence intensity in the confocal volume ($\sim 1\ \mu m^3$) are attributed to the translational diffusion of the fluorophore only and were analyzed using the following auto-correlation function $G(t)$:[44]

$$G(t) = G(0)\left(1 + \frac{t}{\tau}\right)^{-1}\left(1 + \frac{t}{p^2\tau}\right)^{-0.5} \qquad (25)$$

where $G(0)$ is the value of $G(t)$ at time $t = 0$, τ is the diffusion time of the dye within the confocal volume, and p is the structure parameter (ratio of the transversal, ω_{xy}, to longitudinal, ω_z, radius of the confocal volume: $p = \omega_z/\omega_{xy}$). Values of p were obtained from the calibration of the apparatus with R6G, which has a known diffusion coefficient of 2.8×10^{-6} cm^2 s^{-1} in water.[45] Diffusion coefficients (D) were then calculated from measured diffusion times using the following equation:[46]

$$D = \frac{\omega_{xy}^{\ 2}}{4\tau} \qquad (26)$$

Each reported D value is the mean of 10 measurements that were obtained at three or more different locations within the same gel piece to verify its homogeneity on the scale of the confocal volume and to ensure representative values for D. Acquisition times of 20 to 200 s were used to improve the signal-to-noise ratio. The aggregation of peat HA was observed in water at $\mu > 10^{-2}$ (NaCl).

3.3. Measurement of Diffusion Coefficients with the Diffusion Cell. Diffusion coefficients of tritiated water (HTO), Cd^{2+}, Cu^{2+}, Pb^{2+}, and Tl^+ in the agarose hydrogel were determined using diaphragm diffusion cells made of two plastic compartments (source and receiving) connected by the gel; the solution in the two compartments was stirred with a Teflon rod at rates determined with a digital tachometer (VWR, Traceable). Measurements of diffusion coefficients were performed in solutions of various electrolyte (NaCl or $NaNO_3$) concentrations. In a typical diffusion experiment with HTO or ^{109}Cd, an identical volume (200 mL) of the same solution was introduced into both compartments; at time 0, a small volume of tracer (0.2−0.3 mL of an HTO or ^{109}Cd solution with sufficient activity) was added to the source compartment, and an identical volume of the same solution without the tracer was added to the receiving compartment. Prior to an experiment, the gel installed in the diffusion cell had been left to equilibrate overnight under constant stirring with the same solution but without the tracer; this solution was replaced for the experiment. At appropriate time intervals (5 to 10 min), 1-mL samples were taken from each compartment. The ^{109}Cd samples were transferred into 5-mL tubes and counted using a 1480 Wizard gamma counter; the HTO samples were transferred into 7-mL plastic scintillation vials containing 4 mL of ecolume and analyzed with a Winspectral α/β 1414 liquid scintillation counter. For experiments with cold Cd^{2+}, Cu^{2+}, Pb^{2+}, and Tl^+, both compartments were filled with the same solution of electrolyte. After 2 h of equilibration, a small aliquot (0.2 mL) of the metal mixture was introduced into the source compartment, and small samples (0.4 mL) were collected from both compartments at regular time intervals over 3 h for metal measurement by inductively coupled plasma mass spectrometry (ICP-MS; Hewlet-Packard, model 4500). When the same piece of gel was used for several experiments, a dextran blue (MW $\approx$ 2000 kD, Sigma, hydrodynamic radius $\approx$ 15 nm) solution was used to detect leakage, and the cell was filled and left overnight with a solution of electrolyte ([NaCl] = 0.01 M) to remove metal ions. Preliminary diffusion experiments were carried out with HTO at various stirring rate to determine the minimum stirring rate at which the thickness of the diffusive boundary layer became negligible compared to that of the gel. Temperature and pH were measured at the beginning and the end of the experiments and did not vary by more than 1 °C and 0.2 pH units, respectively.

3.4. Determination of Partition Coefficients. Pieces of agarose gel were left to equilibrate for 4 days in various solutions containing metal ions, dyes, and electrolytes. Measureing solute (dye, metal ion or anion) concentrations in the solution provided $[A]_w$. The value of $[A]_g$ was obtained either by measuring [A] in the eluate of the gel or from the difference between measurements of [A] in the initial and final solutions. The partition coefficient (Φ) was then calculated with eq 1. The elution of metals (Na, Li, Al, and Ca) was done with concentrated HNO_3 (Baker, trace metal analysis grade). Metal ion concentrations were determined by atomic absorption spectrometry (Pye Unicam SP9) or ICP-MS; dye concentrations, by UV−vis spectrometry (Perkin-Elmer λ-7 spectrophotometer) or fluorescence (Jasco FP 750 Omnilab); and F^- and Cl^- concentrations, by potentiometry (Orion Research 157205 ion-selective electrode and silver electrode, respectively).

3.5. pH Titrations. Acid−base titrations of dried agarose (0.272 g in 40 mL) were carried out in a glass vessel at $T = 20$ °C and $\mu = 0.1$ (NaCl) under a N_2 atmosphere and vigorous stirring. The suspension was acidified to pH 2.50 (HCl) at least 30 min before titration began. Aliquots of standardized KOH (0.096 M) or HCl (0.100 M) were added using a Soccorex micropipet, and pH was measured with a glass electrode (Metrohm 6.0228.000) using a Metrohm 744 pH meter calibrated with a standardized HCl solution ($\mu = 0.1$). The concentrations of sites and the acidity constant were extracted from the data (70 points per curve) with the optimization program SUPERQUAD,[47] which uses a Marquardt algorithm. A value of $pK_w = 14.0$ was used for the ion product of water.

4. Results and Discussion

4.1. Characterization of the Agarose Gel. Earlier studies have identified "bound" and "free" water[48,49] in gels. Bound water is considered to be strongly associated with the polymer chains by H bonding or by dipole−dipole interactions. Free water has the same properties as normal water. The thermogram obtained by DSC for the agarose gel showed only one fusion peak at temperatures greater than 0 °C, from which we calculated that 91% of the total water of the hydrogel is freezable. However, the heat of fusion value ($\Delta H_{fus} = 6.008$ kJ mol^{-1}, i.e., that for normal water) used to compute the amount of freezable water should be considered to be an upper limit;[48] therefore, the proportions of freezable water are likely underestimated. Thus, these results from DSC suggest that there is little bound water in our agarose hydrogel.

No difference in the IR spectra was observed between oven-dried and lyophilized agarose gels; they showed the presence

of carboxylate (1645 cm^{-1}) and sulfoxide (1380 cm^{-1}, large peak) groups. It was impossible to make a distinction between the sulfonate or sulfinate groups on the basis of these spectra.

Metal analyses of acid-hydrolyzed agarose showed that the major cations are Na^+, Al^{3+}, and Ca^{2+} at concentrations of $(5.5 \pm 0.1) \times 10^{-2}$, $(1.3 \pm 0.1) \times 10^{-3}$, and $(6.1 \pm 0.1) \times 10^{-4}$ mol/kg of dry agarose, respectively. No Cl^- ion was detected from the ionic chromatography of agarose gel samples equilibrated with water. The maximum charge density in the gel (i.e., $Q_{max} = (6.1 \pm 0.1) \times 10^{-2}$ mol/kg of dry agarose; $\rho_{max} = -5.9 \times 10^3$ C/kg of dry agarose; $\rho_{max} = -79$ C/kg of agarose gel) was computed from the sum of the major cations, assuming overall neutrality in the agarose. From the titration curves (Figure S1, Supporting Information), we obtained a concentration of $(5.4 \pm 0.1) \times 10^{-2}$ mol of anionic sites per kg of dry agarose. This result indicates that 90% of the anionic sites have been titrated on the basis of pH. The remaining 10% corresponds roughly to sulfur derivative groups. The value of the intrinsic constant for the protonation of sites extracted from the titration curve is $\log K_a^{int} = 3.9 \pm 0.1$ ($\mu = 0.1$ (NaCl), 20 °C, $\psi \equiv 0$). This value is larger than that of pyruvic acid ($\log K_a = 2.45$[50]) but similar to that of 3-hydroxy-1-oxobutane-1,3-dicarboxylic acid ($\log K_a = 3.54$[51]), indicating that the sites are agarobiose-substituted pyruvic acid; this agrees with the assumption that pyruvate is the major ionic group present in agarose. Given the countercations required to compensate the anionic sites, the minimum ionic strength inside the agarose gel if all ions pairs are dissociated is 8.8×10^{-4}. From the charge density of the gel, its fiber fraction, and the molecular weight of an agarobiose monomer, we calculated that a binding site S is present every 50 agarobiose units in the agarose polymer. Assuming that an agarose fiber is the assembly of six double helixes with a 1.9-nm pitch (involving 36 monomer units) and a 1.5-nm fiber radius,[52] we calculated an average distance of 2.6 nm between two S sites in the fiber. The corresponding calculated area/surface charge $= -24.4$ nm^2, assuming that the negative charges of agarose are spread over the cylindrical fibers' surface.

4.2. Donnan Potential in the Gel: Influence of pH and μ. When agarose gels are exposed to solutions of electrolytes such as NaCl and LiF, only electrostatic interactions should occur inside the gel (i.e., $\theta = \alpha = 1$) because Na^+ and Li^+ are small compared to the pore size of the gel and have a low affinity for the sites; in such cases, ψ can be calculated with either eq 3 (using partition coefficients) or eq 4 (using charge density).

Two empirical relationships ($R^2 \approx 0.9998$) were found between the added salt concentration, $[salt]_{add}$, and the electrolyte concentration, c, (which is the average concentration of both positive and negative ions) in the aqueous phase at equilibrium for identical volumes of gel and external solution over the range of $[salt]_{add} = 10^{-5}-10^{-1}$ M:

$$\log c = -0.07202 + 0.89876 \times \log[NaCl]_{add} - 0.0802 \times (\log[NaCl]_{add})^2 + -0.01961 \times (\log[NaCl]_{add})^3 \quad (27a)$$

and

$$\log c = 0.91178 \times \log[LiF]_{add} + 0.00639 \quad (27b)$$

where $[NaCl]_{add}$ and $[LiF]_{add}$ are the concentrations of NaCl and LiF initially added to the solution, respectively.

In the first approach to the calculation of ψ, the partition coefficient (Φ) of Na^+ or Li^+ was assumed to be equal to π in eq 3, whereas in the second approach the value of c in eq 4 was computed with eqs 27a and 27b.

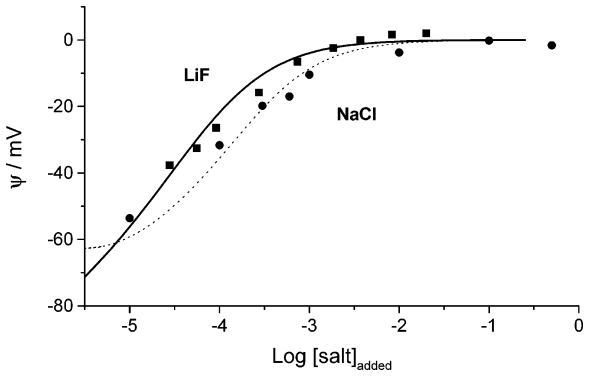

Figure 1. Donnan potential computed with eq 3 from partition coefficients of (■) Li^+ and F^- and (●) Na^+ and Cl^- as a function of salt concentration added to the binary system of agarose gel−water, (1:1 υ). The lines (—, LiF; - - -, NaCl) are predictions obtained with eq 4 using eqs 28a and 28b for c and $\bar{\rho} = -73$ C/kg.

Figure 1 shows plots of ψ obtained with eq 3 (filled dots or squares) as a function of the added salt concentration. These experimental values were fitted with eqs 4 and 27a or 27b (solid and dotted lines in Figure 1), and an average value of $\rho_{max} = -73$ C/kg of agarose gel was obtained, which is in good agreement with the value obtained from potentiometric titrations: $\rho_{max} = -79$ C/kg. Figure 1 shows excellent agreement between ψ values obtained from the partitioning of ions and those predicted from the charge density of the agarose gel. For the same given value of $[salt]_{add}$, ψ is smaller for LiF than for NaCl because Li^+ has a higher charge density than Na^+, which equilibrates the charges of the gel more efficiently.

Charge density and ψ can be expressed as a function of pH and μ as described below. The intrinsic equilibrium constant for the formation of protonated pyruvate groups, K_a^{int}, is

$$K_a^{int} = \frac{Q_{PyH}}{(Q_{Py^-})[H]_p} = \frac{Q_{PyH}}{(Q_{Py^-})[H]_w} \exp\left(-\frac{F\psi}{RT}\right) = K_a^{app} \exp\left(\frac{F\psi}{RT}\right) \quad (28)$$

where $[H]_p$ and $[H]_w$, are the concentrations of H^+ in the pores of the gel and in the external solution, respectively, K_a^{app} is the apparent equilibrium constant, and $[H]_p$ is related to $[H]_w$ by the Boltzmann equation:

$$[H]_p = [H]_w \exp\left(-\frac{F\psi}{RT}\right) \quad (29)$$

Combining eq 28 with the mass balance for pyruvate groups

$$Q_{Py}^{\ t} = Q_{P_{y^-}} + Q_{PyH} \quad (30)$$

gives

$$\frac{Q_{Py^-}}{Q_{Py}^{\ t}} = \frac{1}{1 + 10^{-(pH_p - 3.9 + \log \gamma_H)}} \quad (31)$$

where Q_{PyH} is the concentration of protonated pyruvate groups. γ_H, the activity coefficient of H^+, is a function of μ and can be computed by several equations.[53] Substituting eq 31 into eq 5, where Q is the sum of negatively charged pyruvate (Q_{Py^-}) and sulfonic (Q_{SO_3}) groups, gives

$$\frac{\rho}{F} = Q_{SO_3} + Q_{Py^-} = Q_{SO_3} + \frac{Q_{Py}^{\ t}}{1 + 10^{-(pH_p - 3.9 + \log \gamma_H)}} \quad (32)$$

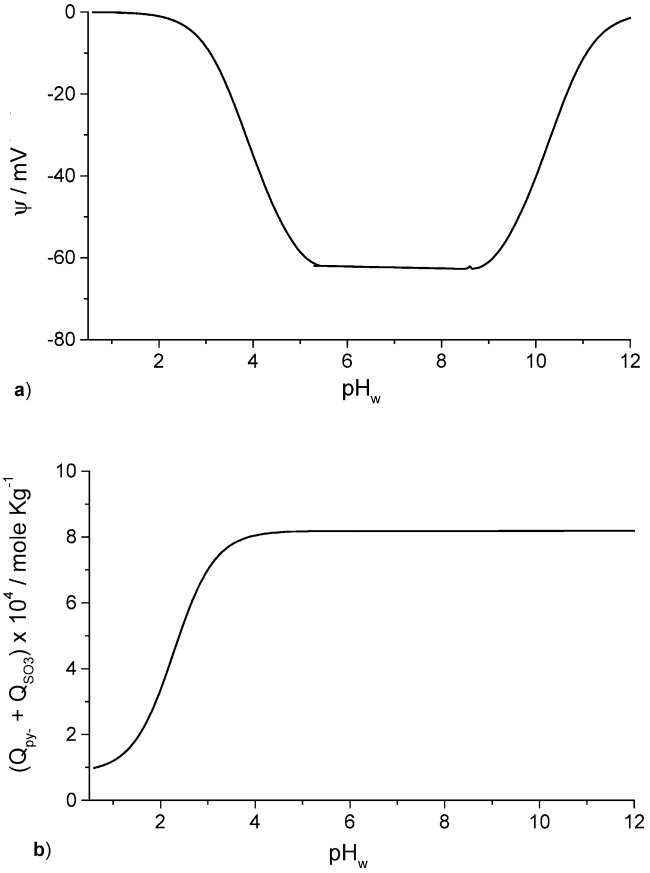

Figure 2. (a) Donnan potential (calculated with eq 33) and (b) charge density (calculated with eq 32) vs pH for the agarose gel (see text, section 4.2).

and combining eqs 4 and 32 leads to

$$\Psi = \frac{RT}{F}\sinh^{-1}\left(\frac{1}{2c}\left(Q_{SO_3} + \frac{Q_{Py}{}^{t}}{1 + 10^{-(pH_p - 3.9 + \log \gamma_H)}}\right)\right) \quad (33)$$

pH_p can be obtained from the proton mass-balance equation for protons for the alkalimetric titration of the gel

$$[H]_p M_g + Q_{PyH} M_g + [H]_w V_w = [H]_w{}^{i} V_w - [OH]_{add} V_{add} \quad (34)$$

after the proper correction for ionic strength with activity coefficients. In eq 34, M_g is the mass of hydrogel, V_w is the volume of external solution in equilibrium with the gel, $[H]_w{}^{i}$ is the initial concentration of H^+ in the external solution, and V_{add} and $[OH]_{add}$ are the volume ($V_{add} \ll V_w$) and concentration of added NaOH, respectively. Figure 2 displays plots of ρ/F ($= Q_{SO_3} + Q_{Py^-}$; computed with eq 32) and ψ (computed with eq 33) as a function of pH for the agarose gel when no electrolyte other than the titrant is added. It shows that the gel bears its maximum charge at pH > 3.5 (Figure 2b) and that the influence of this charge is maximized at 5 < pH < 9 and decreases beyond these boundaries (Figure 2a) because of the screening effect of the increasing ionic strength required to modify the pH values.

4.3. Partitioning of the Electrolytes Between the Aqueous Solution and the Agarose Gel. The partition coefficients, Φ, of the ions of electrolytes LiF and NaCl between the agarose gel and the external solution (eq 1) are shown in Figure 3. They were determined at pH 6, at which the gel sites S are fully deprotonated. Because the ions of these electrolytes are not

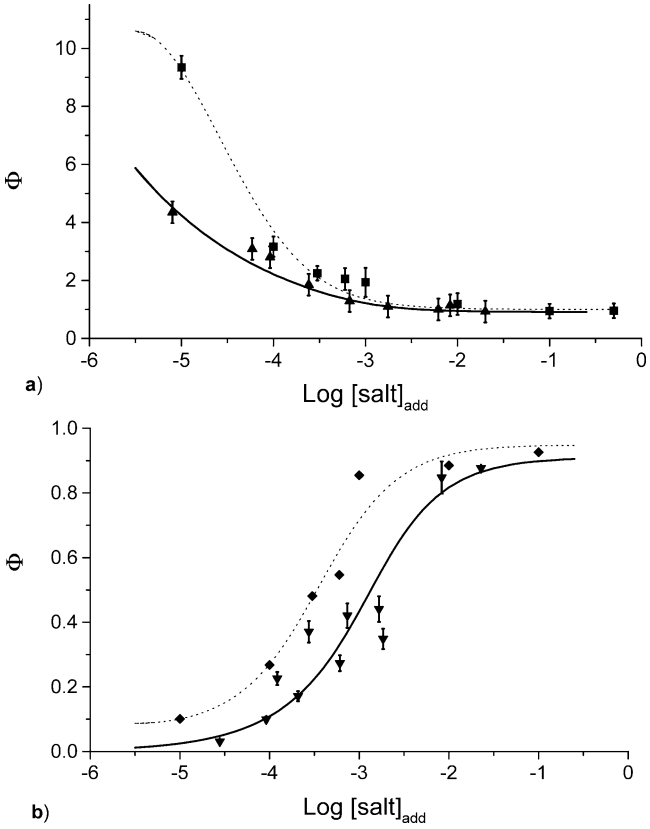

Figure 3. Partition coefficients of ions obtained with eq 1 as a function of added NaCl or LiF concentrations. (a) Na^+ (■), Li^+ (▲); (b) Cl^- (◆) and F^- (▼). The lines are predictions obtained with eq 35 (- - - for Na^+ and Cl^-; — for Li^+ and F^-). $T = 20$ °C; pH = 6.

specifically bound to S sites ($\alpha = 1$), the total charge density of the gel is not affected by these ions, and the value of Φ reflects essentially steric and electrostatic interactions (θ and π in eq 1). The expression for Φ, obtained by combining eqs 1, 3, and 4, is

$$\ln \Phi = \ln \theta - z_A \times \sinh^{-1}\left(\frac{\rho}{2Fc}\right) \quad (35)$$

Figure 3 shows that the prediction of Φ, obtained with eq 35, agrees with the experimental values of Φ. The variations in Φ with the concentration of electrolyte clearly shows the effect of electrostatic interactions on the retention of ions in the gel. Attractive (Figure 3a) and repulsive (Figure 3b) interactions occur with cations and anions, respectively, because the gel is negatively charged. The strength of these interactions decreases with increasing ionic strength because the hydrogel charges become screened.

4.4. Partitioning of Trace Compounds between the Aqueous Solution and the Gel. The partition coefficients, Φ, of charged dyes (calcein^{3-}, eosin^{2-}, and R6G^{2+}) as well as HA, peat HA, and trace metals (Cd^{2+}, Cu^{2+}, Hg^{2+}, Pb^{2+}, and Tl^+) (not shown) were measured at pH 6 and at concentrations ($10^{-6} - 10^{-8}$ M) much lower than $[S]_t$ ($[S]_t = 8.8 \times 10^{-4}$ M) and electrolyte concentrations of 10^{-5} to 0.1 M. Under such conditions, $[S] \approx [S]_t$, and π depends only on the electrolyte concentration. According to eq 1, the term $\theta\alpha$ can be calculated from the ratio $^{\Phi}/_{\pi}$, where π is obtained with eqs 3 and 4. The ratio $^{\Phi}/_{\pi}$ is plotted in Figure 4 as a function of the hydrodynamic radius, R_A, of the test ions, and the values of $\theta\alpha$ are given in Table 1. The values of R_A for the fluorescent organic compounds were computed with Stoke's equation from diffusion coefficients

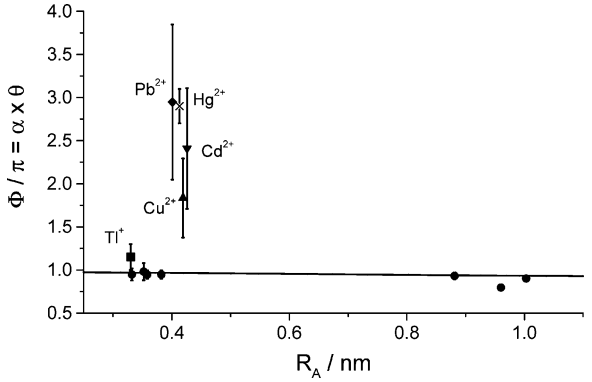

Figure 4. Φ/π ($= \theta \times \alpha$) as a function of the hydrodynamic radius R_A for Cd^{2+} (▼), Cu^{2+} (▲),Tl^{+} (■), Hg^{2+} (×), and Pb^{2+} (◆). A single symbol (●) is used for Li^{+}, F^{-}, Na^{+}, Cl^{-}, $R6G^{2+}$, calcein^{3-}, eosin^{2-}, and HA, which all have a value of Φ lower than 1. The line is the prediction of Φ with eq 2 using $R_p = 36$ nm (Giddings' plot[36]). R_A and the nature and concentrations of electrolytes are given in Table 1. $[A]_{tot} = 3-5 \times 10^{-6}$ M; pH = 6.

TABLE 1: Hydrodynamic Radius of Diffusing Species and Their Corresponding $(\bar{D}_g^A/D_w^A)_{max}$ and $\theta \times \alpha$ Values[a]

solute	R_A/nm	$D_w^A \times 10^6$/ cm^{2}s^{-1}	$\bar{D}_g^A/D_w^A$	$\theta \times \alpha$ ($\pm\sigma$)
HTO	0.142	22.36	0.81	
Na^{+}	0.358[b]			0.94 (0.05)[d]
Li^{+}	0.382[b]			0.95 (0.05)[e]
Cl^{-}	0.332[b]			0.95 (0.07)[d]
F^{-}	0.352[b]			0.98 (0.10)[e]
$R6G^{2+}$	0.744[c]	2.88	0.91[d]	0.93 (0.04)[d]
NB^{2+}	0.610[c]	3.51	0.91[d]	
calcein^{3-}	0.834[c]	2.57	0.88[d]	0.90 (0.03)[d]
eosin^{2-}	0.800[c]	2.60		0.80 (0.03)[d]
peat HA	0.900[c]	2.22	0.87[d]	
HA	0.997[c]	2.15	0.88[d]	0.90 (0.03)[d]
parvalbumin	2.850[c,g]	0.75	0.88	
	3.160[c,h]	0.68	0.85	
ovalbumin	5.400[c,h]	0.40	0.68	
allophycocyanin	5.270[c,g]	0.41		0.74 (0.07)
R-phycoerythrin	6.720[c,g]	0.32	0.62	
	7.260[c,h]	0.295	0.60	
Tl^{+}	0.330[b]	17.50	0.55[f]	1.15 (0.50)[f]
Cu^{2+}	0.419[b]	6.38	0.85[f]	1.83 (0.46)[f]
Cd^{2+}	0.426[b]	6.24	0.76[f]	2.41 (0.70)[f]
$^{109}Cd^{2+}$	0.426[b]	6.24	0.75[d]	
Hg^{2+}	0.413			2.9 (0.2)[f]
Pb^{2+}	0.40[b]	8.22	0.49[f]	2.95 (0.90)[f]

[a] Agarose/H_2O: 1.35% w; $[S^-]_{tot} = 8.8 \times 10^{-4}$ M; $T = 20$ °C; pH 6. [b] From reference 54. [c] Measured in this work by FCS. [d] The electrolyte is NaCl. [e] The electrolyte is LiF. [f] The electrolyte is $NaNO_3$. [g] $\mu = 0.1$. [h] $\mu = 0.01$.

measured by FCS in pure water, whereas the R_A values of metal ions were taken from the literature.[54] Figure 4 and Table 1 clearly show significant specific interactions only for metal ions Cu^{2+}, Cd^{2+}, Hg^{2+}, and Pb^{2+} (and maybe for Tl^{+}), which show $\theta\alpha$ values larger than 1.

Figure 4 and Table 1 indicate that $\theta\alpha$ values for organic dyes allophycocyanin and HA, anions Cl^{-} and F^{-}, and cations Na^{+} and Li^{+} are lower than 1, and it can be assumed that $\alpha \approx 1$ for these ions. Using this assumption, the best fit of eq 2 to these data (Figure 4) yielded $R_p = 36 \pm 3$ nm. Because the probes that were used had a small hydrodynamic radius, the obtained value of R_p should be considered to be an average value of the relatively small pore sizes of the agarose gel. Nevertheless, this value is close to the average value of $\bar{R}_p = 35-47$ nm, obtained from neutron-scattering measurements.[14,55] Because we should have $\Phi \approx \theta\pi$ for these ions, eq 35 should apply, as for

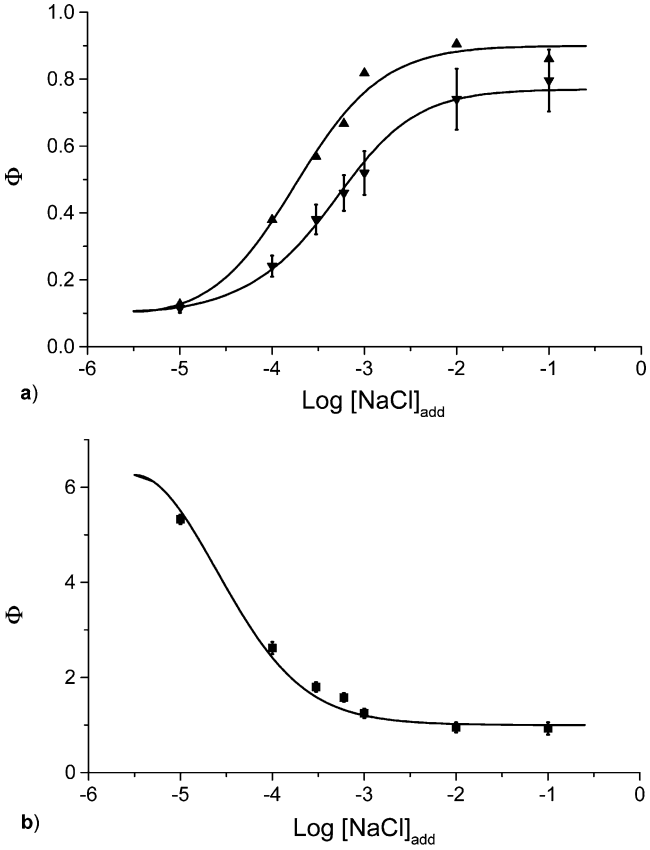

Figure 5. Partition coefficients of calcein^{3-} (▲), eosin yellow^{2-} (▼), and $R6G^{2+}$ (■) as a function of the added NaCl concentration for the agarose gel. The lines are predictions of Φ with eq 36. $[A]_{tot} = 3-5 \times 10^{-6}$ M; pH = 6.

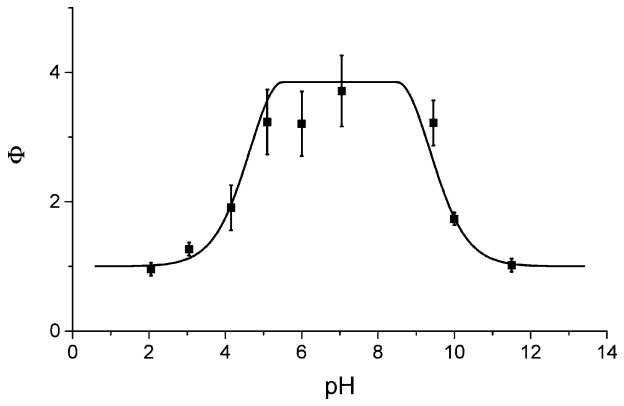

Figure 6. Partition coefficients of $R6G^{2+}$ as a function of pH (■) for the agarose gel. The line is the prediction of Φ with eq 36. $[R6G^{2+}] = 3 \times 10^{-6}$ M was used, and the pH was adjusted with HCl or NaOH.

electrolytes NaCl and LiF. Examples given in Figure 5 for calcein^{3-}, eosin^{2-}, and $R6G^{2+}$ indeed show that eq 35 accurately predicts the partitioning of these solutes as a function of added salt concentration. Figure 6 also shows that eq 35 adequately predicts the effect of pH on the partition coefficient of a trace solute such as $R6G^{2+}$ when no electrolyte other than the titrant is added and confirms the validity of the equation used to compute Figure 2.

For Tl^{+}, Cu^{2+}, Cd^{2+} Hg^{2+}, and Pb^{2+}, Figure 4 and Table 1 indicate a contribution from specific chemical interactions ($\alpha > 1$) to the partition coefficient of these cations in addition to the nonspecific electrostatic interactions. Equation 9 allows the term K_A^{int} [S] to be obtained from the experimental values of Φ provided that π is known. For each metal ion, we computed

TABLE 2: Comparison of the Intrinsic Equilibrium Constants (log $K_A^{int}(\pm\sigma)$) for the Formation of Metal Complexes with Sites in the Agarose Gel with Equilibrium Constants for the Formation of Metal Complexes with Pyruvic Acid Groups (log K_{Pyr})[a]

	log K_A^{int} ($\pm\sigma$)		
ion	from Φ	from $\bar{D}_g^A/D_w^A$	log K_{Pyr}
Tl^+	**2.7** (0.1)	**2.92** (0.06)	
Cu^{2+}	**3.1** (0.1)	**2.4** (0.2)	2.76[b]
Cd^{2+}	**3.2** (0.2)	**2.6** (0.1)	2.96[c]
Hg^{2+}	**3.4** (0.2)		
Pb^{2+}	**3.5** (0.2)	**3.1** (0.1)	

[a] Agarose/H_2O: 1.35% w; $[S^-]_{tot} = 8.8 \times 10^{-4}$ M; $T = 20$ °C; pH 6; electrolyte, $NaNO_3$. [b] The ligand is parapyruvic acid, $\mu = 0.5$; $T = 25$ °C.[59] [c] The ligand is phosphenoylpyruvic acid, $\mu = 0.1$; $T = 25$ °C.[60]

π from eqs 3 and 4 and plotted $^1/_\Phi$ as a function of $^1/_\pi$ (Figure S2, Supporting Information) to obtain a relatively homogeneous distribution of experimental data. The slope from these curve is $^1/_\alpha$ ($= 1/(1 + K_A^{int}[S])$), from which we obtained the K_A^{int} values given in Table 2.

Values for the formation constants of pyruvic acid complexes with metal ions are very scant. The magnitude of the interactions between the gel and the metal ion increases from Tl^+ to Pb^{2+}, as expected from simple hard acid−base considerations. The values available for Cu^{2+} and Cd^{2+} are of the same order of magnitude as the apparent binding constants obtained in this study from the partition coefficients of these metal ions (Table 2), although somewhat lower. The gel is formed from fibers comprising bundles of agarose macromolecules.[52] The average distance calculated between two pyruvate groups in the fiber (2.6 nm) is small. Thus formation of a S_2A complex between two polymer chains, which would increase the apparent binding constant, cannot be excluded.

4.5. Effects of Specific and Nonspecific Interactions on the Diffusion of Solutes in the Agarose Gel. To give a better indication of the solute−gel interactions, this section reports the ratio $\bar{D}_g^A/D_w^A$, where D_w^A is the diffusion coefficient of solute A in water. The $\bar{D}_g^A$ values of the organic dyes were obtained by direct FCS measurements in the gel, whereas for the trace metal ions and HTO they were obtained indirectly, from the transport of these solutes from the source to the receiving solution in a diffusion cell. Figure S3 (Supporting Information) shows that [A] increases linearly in the receiving solution of the diffusion cell during the course of a typical experiment. The linear increase of [A] in the receiving solution begins after a lag period due to the establishment of a linear concentration gradient across the gel; the length of this lag period depends on the time required for A to equilibrate with the binding sites in the gel. Linearity in [A] is maintained as long as the concentration gradient of [A] across the gel remains constant (steady-state regime) (i.e., when the concentration in the source does not change appreciably with time and remains much larger than that in the receiving solution). The values of $\bar{D}_g^A$ discussed below were obtained with eq 19 from the linear part of plots of [A] versus time in the receiving solution (Figure S3). In particular, combining eqs 1 and 19 gives

$$\frac{\bar{D}_g^A}{D_w^A} = \frac{sm}{D_w^A sm\Phi C_s^A} = \frac{sm}{D_w^A sm\theta\pi\alpha C_s^A} \qquad (36)$$

We discuss below the ratio $\bar{D}_g^A/D_w^A$ rather than the value of $\bar{D}_g^A$ to give a better indication of the solute−gel interactions.

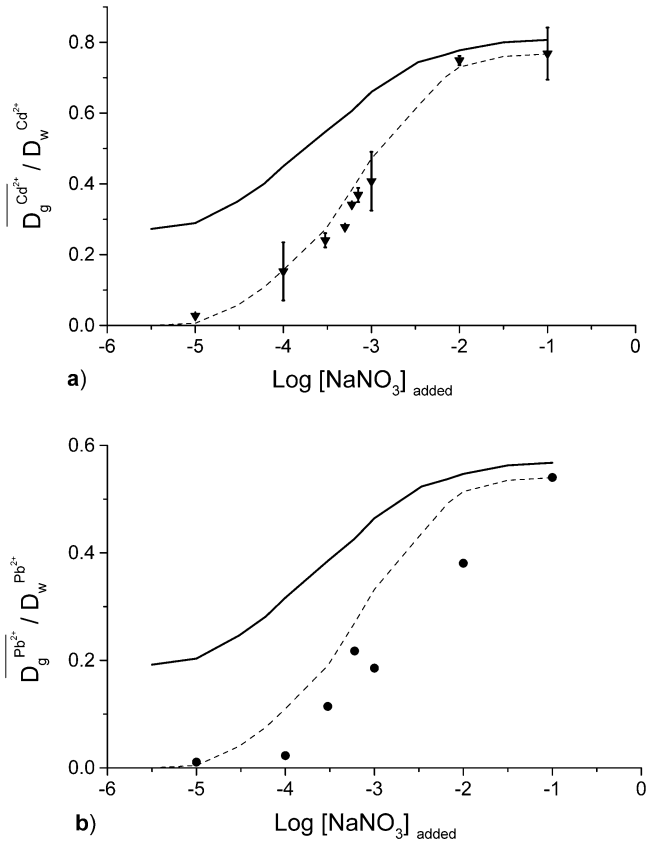

Figure 7. $\bar{D}_g^A/D_w^A$ for (a) Cd^{2+} (▼) and (b) Pb^{2+} (●) as a function of the added salt concentration. The lines are the predictions from SPB theory[34,31] using eqs 21 and 22 (full line, cylindrical cell) or eqs 23 and 24 (- - -, spherical cell). $T = 20$ °C; $[M^{n+}]_{tot} \approx 10^{-6}$ M; $V_w = 200$ mL; $V_{gel} = 0.26$ mL; pH ~6; $b = 1.5$ nm; cylindrical cell: $a = 38.5$ nm; area/surface charge $= -24.42$ nm^2; spherical cell: $a = 12.5$ nm; area/surface charge $= -28.27$ nm^2.

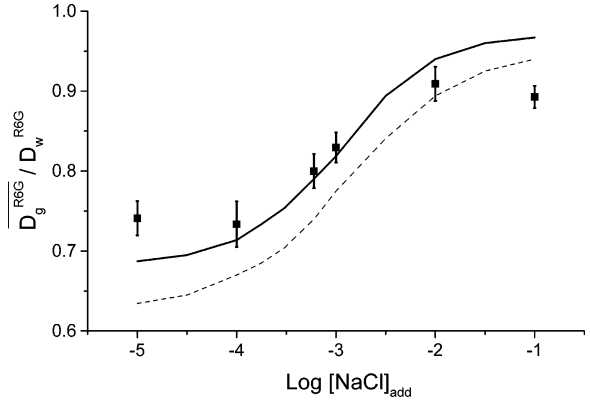

Figure 8. $\bar{D}_g^{R6G}/D_w^{R6G}$ vs $[NaCl]_{add}$ in a system composed of gel only. The lines are the predictions from SPB theory[34,31] using eqs 21 and 22 (—, cylindrical cell) or eqs 23 and 24 (- - -, spherical cell). $T = 20$ °C; $[R6G]_{tot} = 2 \times 10^{-8}$ M; $[S]_{tot} = 8.2 \times 10^{-4}$ M; pH = 6; $b = 1.5$ nm; cylindrical cell: $a = 38.5$ nm; area/surface charge $= -24.42$ nm^2; spherical cell: $a = 12.5$ nm; area/surface charge $= -28.27$ nm^2.

Figures 7, 8, and S4 (Supporting Information) show that values of $\bar{D}_g^A/D_w^A$ for Tl^+, Cu^{2+}, Cd^{2+}, Pb^{2+}, and $R6G^{2+}$ increase with the concentration of added salt and tend to a limiting value $(\bar{D}_g^A/D_w^A)_{max}$ at which the electrostatic interactions are fully screened ($\mu \geq 0.01$). The ratio $(\bar{D}_g^A/D_w^A)_{max}$ falls in the range of 0.4−0.9, depending on the metal ion (plateaus in Figures 7, 8, and S4). The plot of $(\bar{D}_g^A/D_w^A)_{max}$ as a function of R_A (Figure 9) shows that the studied solutes are divided into two groups. The solutes in the first group (R6G, NB, calcein,

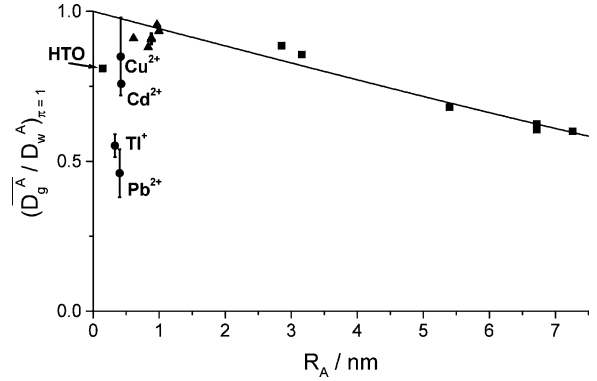

Figure 9. $\bar{D}_g^A/D_w^A$ (when $\pi = 1$) as a function of the hydrodynamic radius R_A for Cd^{2+}, Cu^{2+}, Tl^+, and Pb^{2+} (●) and for $R6G^{2+}$, NB^{2+}, calcein^{3-}, HA, peat HA (▲), and proteins (■). The line is the prediction of $\bar{D}_g^A/D_w^A$ with eq 3 using $R_p = 37$ nm (Renkin's plot[38]). For the values of $\bar{D}_g^A/D_w^A$ (when $\pi = 1$), see Table 1.

HA, peat HA, parvalbumin, ovalbumin, and *R*-phycoerythrin) have values of $(\bar{D}_g^A/D_w^A)_{max}$ (Figure 9 and Table 1) that agree with the previous finding (section 4.4) that these solutes have no specific interactions with the gel. Fitting eq 11 to this group of data yields an average value of $R_p = 37 \pm 2$ nm, which is similar to that of 36 ± 3 nm obtained by fitting eq 2 to the partition coefficients (section 4.4). The second group (HTO, Tl^+, Cd^{2+}, Cu^{2+}, and and Pb^{2+}) shows lower values of $(\bar{D}_g^A/D_w^A)_{max}$ (0.49−0.85; Figure 9 and Table 1) than those of solutes with comparable sizes for which only steric effects are important, that is, 0.94−0.98 (see the line in Figure 9 and $\theta\alpha$ data in Table 1). These low values of $(\bar{D}_g^A/D_w^A)_{max}$ suggest chemical interactions of these solutes with the agarose gel. For HTO, the observed $\bar{D}_g^A/D_w^A$ value (0.81) is lower than expected on the basis of steric effects only (0.98) because of specific interactions of water with the agarose fibers via hydrogen bonding; this reduction of the value of $\bar{D}_g^A/D_w^A$ for HTO is consistent with the finding from DSC measurements, which indicates that about 10% of HTO is bound in the agrose gel (section 4.1). For metal ions, the low ratios can be attributed to a specific association with binding sites S, as already observed in partitioning experiments. Then, in absence of electric field effects, the intrinsic equilibrium constant for the formation of complexes (K_A^{int}) can be calculated by combining eqs 10 and 17:

$$\left(\frac{\bar{D}_g^A}{D_w^A}\right)_{max} = \frac{\sigma}{1 + K_A^{int}[S]} \qquad (37)$$

In principle, the variation of $\bar{D}_g^A/D_w^A$ with μ can be used to evaluate the electrostatic effect on diffusion according to SPB theory (Figures 7 and S4, solid and dashed lines). However, in practice, experimental errors associated with the determination of $\bar{D}_g^A/D_w^A$ for trace metals may be a limitation of these interpretations for several reasons. First, the ratio $\bar{D}_g^A/D_w^A$ for trace metals is obtained indirectly from the transport of these metals from the source to the receiving solution. During this process, the transfer step at the water−gel interface on each side of the membrane may play a significant role because of differences in gel structure in the bulk gel and at the interface. In addition, the determination of $\bar{D}_g^A/D_w^A$ requires an important correction for the π parameter, which is obtained from the measurement of Φ. All of these operations may result in the accumulation of the trace metal results in terms of SPB theory. It may explain why consistent predictions with SPB are not observed in Figures 7 and S4. In contrast, the diffusion

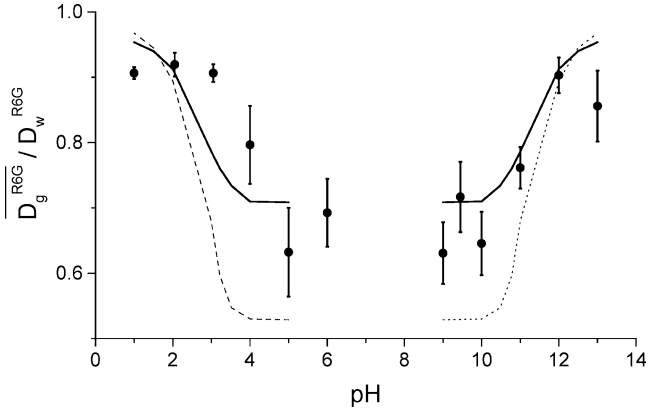

Figure 10. Ratio D_g^{R6G}/D_w^{R6G} vs pH for the agarose gel. The lines are the predictions with the SPB theory,[34,31] using eqs 21, 22 (full line, cylindrical cell) or eqs 23, 24 (dashed line, spherical cell). $T = 20$ °C; $[R6G]_t \approx 2 \times 10^{-8}$ M; $[S]_{tot} = 8.2 \times 10^{-4}$ M; $V_w/V_g = 1$; $b = 1.5$ nm; cylindrical cell: $a = 38.5$ nm; area/surface charge $= -24.42$ nm^2; spherical cell: $a = 12.5$ nm; area/surface charge $= -28.27$ nm^2.

coefficient of $R6G^{2+}$ was measured directly within the gel by FCS, and no correction factor had to be applied. For this reason, testing the relevancy of the cell shape used in the SPB modeling should be given more credibility for $R6G^{2+}$ than for the metals.

Table 2 reports the values of K_A^{int} for the metals obtained with eq 37. A comparison of these values with those obtained from the measurements of metal partitioning indicates that both sets of values agree within less than an order of magnitude. Modeling of the ionic strength effect on $\bar{D}_g^A/D_w^A$ of the metals with SPB theory displays the same trend observed for the measured values of $\bar{D}_g^A/D_w^A$ for the metal ions (Figures 7 and S4) and for R6G (Figure 8), suggesting that electrostatic attraction with agarose fibers reduces the diffusion of metal ions. Use of the spherical cell geometry gives a better prediction of the experimental data than the cylindrical geometry, which systematically overestimates the ratio.

R6G carries two positives charges, and its apparent diffusion coefficient in the gel (D_g^{R6G}) is reduced by 20−30% when $[salt]_{add}$ decreases from 10^{-2} to 10^{-5} M for gel alone and a binary system made of identical volumes of gel and water, respectively (Figures 8 and 10). When electrostatic interactions are completely screened in the agarose gel (i.e., $\mu \geq 10^{-2}$), the measured diffusion coefficient of R6G within the gel is $(0.91 \pm 0.05) \times D_w^{R6G}$. Because measurements of partition coefficients have shown that there is no specific interactions between $R6G^{2+}$ and the gel (section 4.4; Figure 5), values of D_g^{R6G}/D_w^{R6G} lower than 1 are attributed to tortuosity effects or steric hindrance within the gel. We attribute the increase in D_g^{R6G}/D_w^{R6G} with μ to a progressive screening of the electrostatic field in the diffuse layer around the agarose fibers within the gel (section 2.2). The results are in agreement with previous studies[56,57] reporting a decrease in the apparent diffusion coefficients of choline$^+$ and Li^+ in carrageenan and DNA gels. Figures 8 and 10 show qualitative agreement between the variations of D_g^{R6G}/D_w^{R6G} as a function of $\log[salt]_{add}$ obtained experimentally and those values predicted by SPB theory using eqs 20−24. It should be noted that the variations of D_g^{R6G}/D_w^{R6G} with pH when no electrolyte other than the titrant is added (Figure 10) display a screening effect that is similar to that observed from the measurements of partition coefficients (Figure 6). As explained before, the change in D_g^{R6G} (or Φ) with pH is due to the increase in μ by the addition of titrant at 4 > pH > 10, which screens the charges of the gel. Figures 8 and 10 show that cylindrical cell geometry better predicts the experimental

D_g^{R6G}/D_w^{R6G} values than the cylindrical geometry that leads to a systematic underestimation. It also seems that using experimentally determined structural parameters in the cell model gives a better modeling than that with respect to the fiber fraction in the case of this small solute.

Only slight increases in the ratio D_g^A/D_w^A for the two humic acids and calcein^{3-} were observed with increasing salt concentration. The changes in D_g^A/D_w^A for these negatively charged solutes were, however, on the order of 10% (i.e., of similar magnitude to the experimental errors). $(D_g^A/D_w^A)_{max}$ values are 0.9, 0.8, and 0.8 for calcein^{3-}, HA, and peat HA, respectively.

5. Conclusions

We have characterized the nature and the density of fixed anionic binding sites in an agarose hydrogel and have modeled the partitioning of various solutes between the gel and the external solution and the transport of these solutes within the hydrogel. The agarose gel comprises sites bearing a resemblance to pyruvic and sulfonic functional groups with a maximum density of charges of $\rho_{max} = -5.9 \times 10^3$ C/kg of agarose. Modeling takes into account steric, specific, and electrostatic interactions between the agarose gel and solutes; it provides in general good predictions of the observed effects of pH and ionic strength on the partitioning and diffusion of small ions. SPB theory predicts the observed trend in the variation of the experimental values of D_g^A/D_w^A with μ, suggesting that local electrostatic potential influences the diffusion of ions in the gel. Better agreement between the experimental and predicted values would probably be achieved if $\bar{D}_g^A$ were to be measured directly in the gel.

The present results are useful in various applications of agarose gel where pH and ionic strength changes may play important roles such as drug delivery from gel capsules[58] or the use of agarose for in situ environmental analysis (e.g., voltammetric gel integrated microelectrodes[3] or diffusion gradients in thin films[1]). In particular, our results indicate that it is imperative to use calibration solutions with the same ionic strength and pH as those of the test solution when DGT devices are deployed in natural waters with $\mu < 0.01$ to ensure that the diffusion coefficient of the test ion in the gel is the same for the calibration and test solutions.

Acknowledgment. We thank M. Martin, N. Parthasarathy, J.-P. Senn, and M. Blanco for their assistance with ICP-MS, the fluoride ion selective electrode, ionic chromatography, and atomic absorption measurements, L. Bérubé, R. Quirion, and L. Rancourt for technical help with the diffusion cell, F. Bilodeau for the DSC measurements, and N. Parthasarathy, M. L. Tercier, K. Wilkinson, J.-P. Rivera, and H. Van Leuven for helpful discussions. This work was supported by grants from the Swiss National Science Foundation, the Natural Sciences and Engineering Research Council of Canada, the Ontario Power Generating Company, the Mining Association of Canada, and Health Canada (Toxic Substances Research Initiative program). R.R.G. was supported by a postdoctoral fellowship from the Fonds Québécois de Recherche sur la Nature et les Technologies.

Supporting Information Available: A scheme of organic dyes, a potentiometric titration of an aqueous solution of agarose, the value of $^1/_\Phi$ as a function of $^1/_\pi$ for Cd^{2+} ions, concentrations of Cd^{2+} in the diffusion cell versus time during the course of a typical experiment to measure diffusion coefficients in the agarose gel, and $\bar{D}_g^A/D_w^A$ for Tl^+ and Cu^{2+} as a function of the added salt concentration. This material is available free of charge via the Internet at http://pubs.acs.org.

References and Notes

(1) Davison, W.; Zhang, H. *Nature* **1994**, *367*, 546.
(2) Jeppsson, J.-O.; Laurell, C.-B.; Franzen, B. *Clin. Chem.* **1979**, *25*, 629.
(3) Tercier, M.-L.; Buffle, J. *Anal. Chem.* **1996**, *68*, 3670.
(4) Belmont-Hébert, C.; Tercier, M.-L.; Buffle, J.; Fiaccabrino, G. C.; de Rooji, N. F.; Koudelka-Hep, M. *Anal. Chem.* **1998**, *70*, 2949.
(5) Buffle, J. *Complexation Reactions in Aquatic Systems: An Analytical Approach*; Wiley & Sons: New York, 1988.
(6) DeRossi, D.; Kajiwara, K.; Osada, Y.; Yamauchi, A. *Polymer Gels*; Plenum Press: New York, 1991.
(7) Ottenbrite, R. M.; Huang, S. J. *Hydrogels and Biodegradable Polymers for Bioapplications*; Park, K., Ed.; American Chemical Society: Washington, DC, 1996.
(8) Dumitau, S. *Polysaccharides: Structural Diversity and Functional Versatility*; Marcel Dekker: New York, 1998.
(9) The Agarose Monograph, 1982, FMC Corporation.
(10) Araki, C.; Arai, K. *Bull. Chem. Soc.* **1967**, *40*, 1452.
(11) Arnott, S.; Fulmer, A.; Scott, W. E.; Dea, C. M.; Moorhouse, R.; Rees, D. A. *J. Mol. Biol.* **1974**, *90*, 269.
(12) Rees, D. A. *Carbohydr. Chem. Biochem.* **1969**, *24*, 267.
(13) Maaloum, M.; Pernodet, N.; Tinland, B. *Electrophoresis* **1998**, *19*, 1606.
(14) Ouali, L.; Starchev, K.; Kohlbrecher, J.; Buffle, J. To be submitted for publication.
(15) Waki, S.; Harvey, J. D.; Bellamy, A. R. *Biopolymers* **1982**, *21*, 1909.
(16) Pernodet, N.; Maaloum, M.; Tinland, B. *Electrophoresis* **1997**, *18*, 55.
(17) Muhr, A. E.; Blanshard, J. M. V. *Polymer* **1982**, *23*, 1012.
(18) Amsden, B. *Macromolecules* **1998**, *31*, 8382.
(19) Gong, P. J.; Hirota, N.; Kakugo, A.; Narita, T.; Osada, Y. *J. Phys. Chem. B* **2000**, *104*, 9904.
(20) Johnson, E. M.; Berk, D. A.; Jain R. K.; Deen, W. M. *Biophys. J.* **1996**, *70*, 1017.
(21) Zhang, S.; Sun, Y. *AIChE J.* **2002**, *48*, 178.
(22) Johnson, E. M.; Berk, D. A.; Rakesh, K. J.; Deen, W. M. *Biophys. J.* **1995**, *68*, 1561.
(23) Hirota, N.; Kumaki, Y.; Narita, T.; Gong, J. P.; Osada, Y. *J. Phys. Chem. B* **2000**, *104*, 9898.
(24) Mattisson, C.; Roger, P.; Jönsson, B.; Axelsson, A.; Zacchi, G. *J. Chromatogr., B* **2000**, *743*, 151.
(25) Alfaro de la Torre, M. C.; Beaulieu, P. Y.; Tessier, A. *Anal. Chim. Acta* **2000**, *418*, 53.
(26) Sangi, M. R.; Halstead, M. J.; Hunter, K. A. *Anal. Chim. Acta* **2002**, *456*, 241.
(27) Phillies, G. D. J.; Malone, C.; Ullmann, K.; Ullmann, G. S.; Rollings, J.; Yu, L. *Macromol. Rev.* **1987**, *20*, 2280.
(28) Phillies, G. D. J.; Pirnat, T.; Kiss, M.; Teasdale, N.; Maclung, D.; Inglefield, H.; Malone, C.; Rau, A.; Yu, L.; Rollings, J. *Macromol. Rev.* **1989**, *22*, 4068.
(29) Fuoss, R. M. *Polym. Sci.* **1954**, *12*, 185.
(30) Schmitt, A.; Varoqui, R. J. *J. Chem. Soc., Faraday Trans. 2* **1973**, *69*, 1087.
(31) Bell, G. M.; Dunning, A. J. *Trans. Faraday Soc.* **1970**, *66*, 500.
(32) Bell, G. M. *Trans. Faraday Soc.* **1964**, *60*, 1752.
(33) Jönsson, B.; Wennerström, P. G. N.; Linse, P. *Colloid Polym. Sci.* **1986**, *264*, 77.
(34) Nilsson, L. G.; Nordensiöld, L.; Stilbs, P.; Braulin, W. H. *J. Phys. Chem.* **1985**, *89*, 3385.
(35) Johansson, L.; Skantze, U.; Löfroth, J. E. *J. Phys. Chem.* **1993**, *97*, 9817.
(36) Giddings, C.; Kucera, E.; Russell, C. P.; Myers, M. N. *J. Phys. Chem.* **1968**, *72*, 4397.
(37) Rosenberg, R. M. *Principles of Physical Chemistry*; Oxford University Press: New York, 1977.
(38) Renkin, E. M. *J. Gen. Physiol.* **1954**, *38*, 225.
(39) Crank, J. *Mathematics of Diffusion*, 2nd ed.; Clarendon Press: Oxford, England, 1975.
(40) http://www.membfound.lth.se/chemeng1/Prog.html.
(41) Pluen, A.; Netti, P. A.; Rakesh, K. J.; Berk, D. A. *Biophys. J.* **1999**, *77*, 542.
(42) *Food Polysaccharides and Their Applications*; Stephen, A. M., Ed.; Marcel Dekker: New York, 1995.
(43) *American Institute of Physics Handbook*; Gray, D. E., Ed. McGraw-Hill: New York, 1972.
(44) Aragon, S. R.; Pecora, R. *J. Phys. Chem.* **1975**, *64*, 1791.
(45) Magde, E. L.; Elson, E. L.; Webb, W. W. *Biopolymers* **1974**, *13*, 28.

(46) Madge, D.; Elson, E. L.; Webb, W. W. *Biopolymers* **1974**, *13*, 28.
(47) Gans, P.; Sabatini, A.; Vacca, A. *J. Chem. Soc., Dalton Trans.* **1985**, 1195.
(48) Quinn, F. X.; Kampff, E.; Smyth, G.; McBrierty, V. J. *Macromolecules* **1988**, *21*, 3191.
(49) Qu, X.; Wirsen, A.; Albertsson, A.-C. *Polymer* **2000**, *4*, 4589.
(50) Leussing, D. L.; Schultz, D. C. *J. Am. Chem. Soc.* **1964**, *86*, 1195.
(51) Monk, C. B. *J. Chem. Soc., Faraday Trans.* **1987**, *83*, 425.
(52) Djabourov, M. A.; Clark, H. A.; Rowlands, D. W.; Ross-Murphy, S. B. *Macromolecules* **1989**, *22*, 180.
(53) Stumm, W.; Morgan, J. J. *Aquatic Chemistry*, 3rd ed.; Wiley: New York, 1996.
(54) Nightingale, J. R. *J. Phys. Chem.* **1959**, *63*, 1381.
(55) Wilkinson, K. Private communication.
(56) Hohansson, L.; Skantze, U.; Lofroth, J. E. *Macromolecules* **1991**, *24*, 6019.
(57) Hohansson, L.; Skantze, U.; Lofroth, J. E. *J. Phys. Chem.* **1993**, *97*, 747.
(58) Brannon-Peppas, L. *Med. Plast. Biomater.* **1997**, 34.
(59) Wold, F.; Ballow, C. E. *J. Biol. Chem.* **1957**, *227*, 301.
(60) Raghavan, N. V.; Leussing, D. L. *J. Indian Chem. Soc.* **1977**, *54*, 68.